

# Ultra-low-power stress-based integrated photonic phase actuator

Jörn P. Epping<sup>1</sup>, Denys Marchenko<sup>1</sup>, Arne Leinse<sup>1</sup>, Richard Mateman<sup>1</sup>, Marcel Hoekman<sup>1</sup>, Lennart Wevers<sup>1</sup>, Chris G. H. Roeloffzen<sup>1</sup>, Matthijn Dekkers<sup>2</sup>, and René G. Heideman<sup>1</sup>

<sup>1</sup> LioniX International BV, P.O. Box 456, Enschede 7500 AL, The Netherlands

Tel.: +31 53 20 30 053, Fax: +31 53 20 11 303, e-mail: [j.p.epping@lionix-int.com](mailto:j.p.epping@lionix-int.com)

<sup>2</sup> SolMateS BV, Drienerlolaan 5, Enschede 7522 NB, The Netherlands

## ABSTRACT

In this work, we present recent improvements on the stress-optic actuator on the silicon nitride-based waveguide platform (TriPleX) in the telecommunication C-band. In our stress-optic phase modulator the refractive index of the waveguiding materials is controlled by the stress-optic effect induced by actuating a 2  $\mu\text{m}$  thick PZT (lead zirconate titanate) layer on top of the TriPleX waveguide geometry. The efficiency of the modulator is optimized by, amongst others, focusing the applied stress in the waveguide core region through a local increase of the top cladding. Using a Mach-Zehnder interferometer, we measured a phase shift of  $\pi$ , i.e. the half-wave voltage,  $V_{\pi}$ , at 12 V and even a phase shift of  $2\pi$  at 25 V at a wavelength of 1550 nm using a modulator with a total length of 15 mm. Even smaller voltages were measured for devices using a reduced top cladding. The measured static power consumption of our stress-optic modulator is well below 1  $\mu\text{W}$  as it is only determined by small leakage currents ( $< 0.1 \mu\text{A}$ ) and, therefore, more than 5 order of magnitude lower than that of conventional thermo-optic phase actuators. The total footprint of the stress-optic actuator is similar to that of thermo-optic actuators due to lower cross-talk to neighboring actuator. These specifications along with minimal excess losses make stress-optic actuator an excellent choice for next generation integrated photonic circuits that require a large number of actuators in silicon photonics in general and in the TriPleX platform in particular.

**Keywords:** Integrated Optics, Microwave Photonics, Actuator, PZT, Silicon nitride, TriPleX<sup>TM</sup>

## 1. INTRODUCTION

For integrated photonics circuits with complex function, such as optical beam forming networks (OBFN) [1,2] or microwave photonic signal processing [3,4], large amounts of phase actuators are mandatory. In the silicon nitride and similar platforms today's phase modulation depends solely on thermo-optic phase shifters[5], which are reliable, straightforward to manufacture, and offer tuning speeds around 1 ms. However, thermo-optic modulators suffer from huge power dissipation, in the order of 300 mW per  $\pi$  phase-shift per modulator, and thermal cross-talk from neighboring heaters. While their tuning speed is sufficient to drive the envisioned applications, the constant power dissipation of thermo-optic modulators makes them less suitable to support large scale waveguide-based matrices.

Recently, we have demonstrated that low-power modulation is feasible for visible light as well as near-infrared light by using stress-optic modulators in the silicon nitride platform[6,7,8]. The stress-optic modulator was realized by harnessing the stress from an actuating piezoelectric material (lead zirconate titanate, PZT) on top of a standard silicon nitride-based TriPleX geometry. The major advantage of such stress-optic modulators over thermo-optic modulators for future applications is their ultra-low power dissipation in a static state, where no high speed tuning is required. The static power consumption is solely determined by tiny leakage currents through the piezoelectric layer resulting in a dissipated power in the  $\mu\text{W}$ -region. Here, we present recent advances in the stress-optic actuator in the telecommunication C-band using the silicon nitride-based waveguide platform, TriPleX. We employ a stress-focusing geometry on top of the waveguide core region, while at the same time allowing for a thinner top cladding to further increase the stress at the waveguide core and keeping the excess loss per modulator minimal. Using a Mach-Zehnder interferometer, we measured a half-wave voltage,  $V_{\pi}$ , at 12 V at a wavelength of 1550 nm using a modulator with a total length of 15 mm.

## 2. STRESS-OPTIC ACTUATOR

We fabricated a stress-optic modulator using a standard double stripe TriPleX<sup>TM</sup> geometry[9], which is also offered via a Process Design Kit (PDK) and Multi Project Wafer (MPW) access. To evaluate the dependence of the stress-optic effect with the top cladding thicknesses,  $t_c$ , we deposited top claddings with a thickness of 2  $\mu\text{m}$  and 3  $\mu\text{m}$  on two wafers. Afterwards a bottom electrode consisting of a 10 nm thick Ti adhesive layer and a 100 nm thick Pt layer was deposited. The PZT layer with  $t_{\text{PZT}} = 2 \mu\text{m}$  was grown on top of this electrode using Solmates SMP-700 pulsed laser deposition (PLD) equipment. PZT deposited by PLD allows for the growth of high-quality layers which has recently become available for large wafer sizes and at commercial throughput[10]. To ensure the quality of the deposited PZT layer, we measured the transverse piezoelectric coefficient,  $e_{31}$ , of -18 to -20 C/m<sup>2</sup>, using

simultaneously produced test structures from the same wafer. Finally, a Pt top electrodes with a thickness of 100 nm were deposited with various widths,  $w$ , and lengths,  $l$ . A scanning electrode microscope (SEM) picture of the resulting structure can be seen in Fig. 1a).

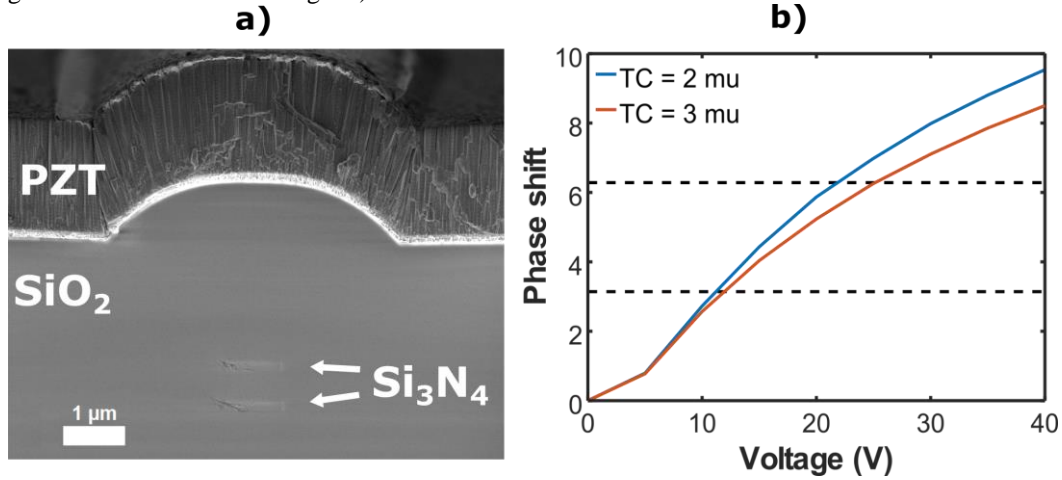


Figure 1. a) SEM picture of the stress-optic actuator on a symmetric double-stripe waveguide with a top cladding of 3 μm and a PZT thickness of 2 μm. b) Phase shift a function of applied voltage for stress-optic actuators analogue to a) with  $l = 1.5$  cm,  $w = 7.5$  μm, and a top cladding thickness (TC) of 2 μm (blue) and 3 μm (orange), respectively. Dashed horizontal lines indicate a applied phase shift of  $\pi$  and  $2\pi$ , respectively.

To determine the phase shift of the stress-optic actuator, we use an asymmetric Mach-Zehnder interferometer filter (aMZI), where a top electrode in one arm was deposited to actuate the PZT layer. The top electrode has a width,  $w$ , of 7.5 μm, which was calculated to give the highest stress in the waveguide core, and a length,  $l$ , of 15 mm resulting in a measured capacitance of the modulator of 3 nF. We used a superluminescent diode with a -3 dB bandwidth of 50 nm at a wavelength around 1550 nm and an optical spectrum analyzer (HP 70951A) to measure the spectral shift in the response of the fabricated aMZI devices with a free spectral range of around 14 nm. To calculate the phase shift of the modulator as a function of voltage we measured the spectral shift for a set of applied dc-voltages, which is shown in Fig. 1 b). We measured a half-wave voltage,  $V_{\pi}$ , (i.e. a phase shift of  $\pi$ ) at 12 V and 11 V for  $t_c = 3$  μm and 2 μm, respectively. A phase shift of  $2\pi$  was measured  $V = 25$  V and 22 V for  $t_c = 3$  μm and 2 μm, respectively. It can be seen that the response of the stress-optic actuator has a proportional regime between 5 and 15 V, for higher voltages the slope of the curve decreases with increasing voltages. The reason for the decrease in modulation strength is the decrease of the transverse piezoelectric coefficient of the PZT layer after it reached its maximum at electric field strengths of around 10 V/μm. This decrease matches with the measured hysteresis-curve of PZT test structures that were fabricated on the same wafer.

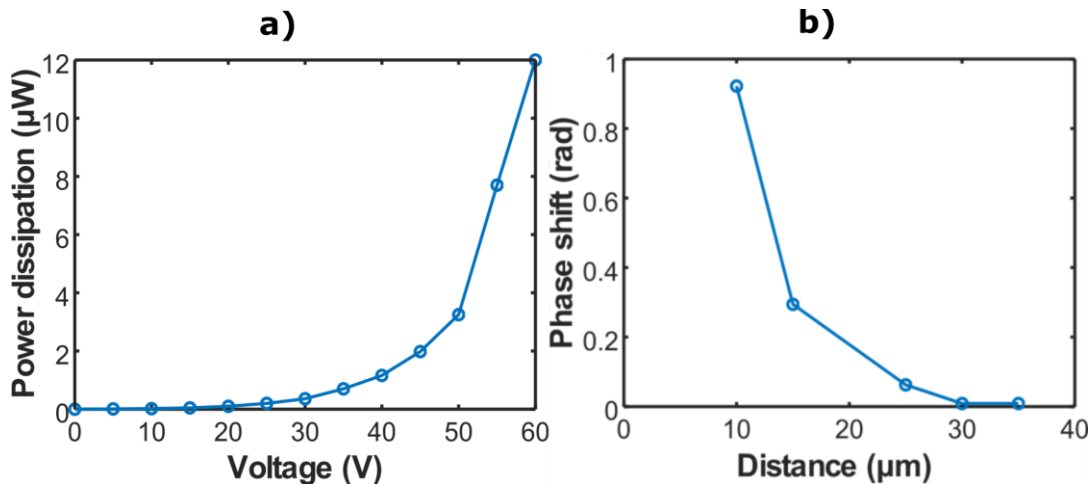


Figure 2. a) Static power dissipation of a stress-optic actuator as a function of applied voltage by measuring the leakage current. The leakage current was measured to be 0.08 μA at 25 V resulting in a power consumption well below 1 μW and went up to 0.2 μA at 60 V ( $P_{diss} = 12$  μW).

To determine the dissipated power of the stress-optic actuator, we measured the leakage current as a function of applied voltage. The calculated dissipated power from this measurement is shown in Fig. 2 a). It can be seen that for voltages needed to reach a full  $2\pi$  phase shift ( $V > 30$  V) the dissipated power is well below 1 μW and, hence, is more than 5 order of magnitude lower than that of thermo-optic actuators. The power consumption of these devices with a driving frequency of 1 kHz (comparable to thermo-optic) is calculated to be below 1 mW [7].

The cross-talk from one actuator to a neighboring device is an important parameter as it provides how densely devices can be packed on a chip. Fig.2 b) shows the measured cross-talk, i.e. induced phase shift, of a stress-optic modulator over a length of 1 cm as a function of distance between the waveguides. It can be seen that the cross-talk decays exponentially with increasing distance and starting from a distance of 30  $\mu\text{m}$  the cross-talk was too low to be measured. The measured cross-talk of the stress-optic actuator is about 8 times smaller when compared to thermo-optic actuators. Due to the small cross-talk stress-optic actuators can be packed more densely on chip and when considering their current length (about 15 mm), stress-optic and thermo-optic actuators have a similar effective device footprint.

### 3. CONCLUSION

In conclusion, we presented the recent improvements on stress-optic modulators for the telecommunication C-band, i.e. a wavelength around 1550 nm, in silicon nitride-based integrated circuits. The measured (static) power consumption characteristics of below 1  $\mu\text{W}$  in the static case, make it an ideal actuator to realize sophisticated optical beamforming networks with 100s and even 1000s of modulators. In this work, we measured a half-wave voltage at 12 V using an electrode with a width of 7.5  $\mu\text{m}$  and a length of 15 mm. The actual footprint of stress-optic modulators is measured to be the same as conventionally used thermo-optic modulators. The increase in modulator length of stress-optic modulators goes in hand with a decrease of cross-talk to neighboring devices when compared with thermo-optic modulators due to the confined actuation of the PZT. To further improve the devices, it is favorable to deposit PZT layers that are thicker than 2  $\mu\text{m}$ . An improved PZT layer thickness should lead to both a higher stress induced into the waveguide core and, as well, an extension of linear modulation regime of the PZT.

### ACKNOWLEDGEMENTS

This project has received funding from the European Union's Horizon 2020 research and innovation program under grant agreement No 688750 (HAMLET) and No 688519 (PIX4LIFE).

This work is supported by NanoNextNL, a micro and nanotechnology consortium of the Government of the Netherlands and 130 partners.

### REFERENCES

- [1] D. Marpaung, C.G.H. Roeloffzen, R.G. Heideman, A. Leinse, S. Sales, and J. Capmany: Integrated microwave photonics, *Laser Photon. Rev.* VOL. 7. pp. 506–538, 2013.
- [2] C.G.H. Roeloffzen, L. Zhuang, C. Taddei, A. Leinse, R.G. Heideman, P.W.L. van Dijk, R.M. Oldenbeuving, D.A.I. Marpaung, M. Burla, and K.-J. Boller: Silicon nitride microwave photonic circuits, *Opt. Express* vol. 21 pp. 22937-22961 2013.
- [3] L. Zhuang, C.G.H. Roeloffzen, M. Hoekman, K.-J. Boller, and A.J. Lowery: Programmable photonic signal processor chip for radiofrequency applications, *Optica* vol. 2 pp. 854-859 2015.
- [4] D. Pérez, I. Gasulla, J. Capmany, and R.A. Soref: Reconfigurable lattice mesh designs for programmable photonic processors, *Opt. Express* vol. 24 pp. 12093-12106 2016.
- [5] D. Pérez, J. Fernández, R. Baños, J.D. Doménech, A.M. Sánchez, J.M. Cirera, R. Mas, J. Sánchez, S. Durán, E. Pardo, C. Domínguez, D. Pastor, J. Capmany, and P. Muñoz: Thermal tuners on a Silicon Nitride platform", arXiv:1604.02958 2016.
- [6] N. Hosseini, R. Dekker, M. Hoekman, M. Dekkers, J. Bos, A. Leinse, and R.G. Heideman: Stress-optic modulator in TriPleX platform using a piezoelectric lead zirconate titanate (PZT) thin film, *Opt. Express* vol. 23 pp. 14018-14026 2015.
- [7] J.P. Epping, D. Marchenko, A. Leinse, R. Mateman, M. Hoekman, L. Wevers, E.J. Klein, C.G.H. Roeloffzen, M. Dekkers, R.G. Heideman: Ultra-low-power stress-optics modulator for microwave photonics, *Proc. SPIE 10106, Integrated Optics: Devices, Materials, and Technologies XXI*, 101060F February 2017.
- [8] W. Jin, E.J. Stanton, N. Volet, R.G. Polcawich, D. Baney, P. Morton, and J.E. Bowers: Piezoelectric tuning of a suspended silicon nitride ring resonator, *IEEE Photonics Conference* October 2017.
- [9] K. Wörhoff, R.G. Heideman, A. Leinse, and M. Hoekman: TriPleX: a versatile dielectric photonic platform, *Adv. Opt. Technol.*, vol. 4 pp. 189–207 2015.
- [10] D.H.A. Blank, M. Dekkers, and G. Rijnders: Pulsed laser deposition in Twente: from research tool towards industrial deposition, *J. Phys. D: Appl. Phys.* vol. 47 pp. 034006 2014.